Contrib Mineral Petrol
DOI 10.1007/s00410-011-0663-y

ORIGINAL PAPER

Evolution of silicic magmas in the Kos-Nisyros volcanic center, Greece: a petrological cycle associated with caldera collapse

Olivier Bachmann · Chad D. Deering · Janina S. Ruprecht · Christian Huber · Alexandra Skopelitis · Cedric Schnyder

Received: 26 February 2011 / Accepted: 9 June 2011

Abstract Multiple eruptions of silicic magma (dacite and rhyolites) occurred over the last ~3 My in the Kos-Nisyros volcanic center (eastern Aegean sea). During this period, magmas have changed from hornblende-biotite-rich units with low eruption temperatures (≤750–800°C; Kefalos and Kos dacites and rhyolites) to hotter, pyroxene-bearing units (>800–850°C; Nisyros rhyodacites) and are transitioning back to cooler magmas (Yali rhyolites). New whole-rock compositions, mineral chemistry, and zircon Hf isotopes show that these three types of silicic magmas followed the same differentiation trend: they all evolved by crystal fractionation and minor crustal assimilation (AFC) from parents with intermediate compositions characterized by high Sr/Y and low Nb content, following a wet, high oxygen fugacity liquid line of descent typical of subduction zones. As the transition between the Kos-Kefalos and Nisyros-type magmas occurred immediately and abruptly after the major caldera collapse in the area (the 161 ka Kos Plateau Tuff; KPT), we suggest that the efficient emptying of the magma chamber during the KPT drew out most of the eruptible, volatile-charged magma and partly solidified the unerupted mush zone in the upper crust due to rapid unloading, decompression, and coincident crystallization. Subsequently, the system reestablished a shallow silicic production zone from more mafic parents, recharged from the mid to lower crust. The first silicic eruptions evolving from these parents after the caldera collapse (Nisyros units) were hotter (up to >100°C) than the caldera-forming event and erupted from reservoirs characterized by different mineral proportions (more plagioclase and less amphibole). We interpret such a change as a reflection of slightly drier conditions in the magmatic column after the caldera collapse due to the decompression event. With time, the upper crustal intermediate mush progressively transitioned into the cold-wet state that prevailed during the Kefalos-Kos stage. The recent eruptions of the high-SiO_2 rhyolite on Yali Island, which are low temperature and hydrous phases (sanidine, quartz, biotite), suggest that another large, potentially explosive magma chamber is presently building under the Kos-Nisyros volcanic center.

Keywords Caldera cycle · Volcanic petrology · Arc magmatism · Aegean arc · Large volcanic eruptions

Communicated by T. L. Grove.

Electronic supplementary material The online version of this article (doi:10.1007/s00410-011-0663-y) contains supplementary material, which is available to authorized users.

O. Bachmann (✉) · C. D. Deering
Department of Earth and Space Sciences,
University of Washington, Box 351310, Seattle,
WA 98195-1310, USA
e-mail: bachmano@u.washington.edu

Present Address:
C. D. Deering
Department of Geology, University of Wisconsin,
800 Algoma Blvd., Oshkosh, WI 54901-8649, USA

J. S. Ruprecht
Lamont-Doherty Earth Observatory of Columbia University,
61 Route 9 W, Palisades, NY 10964, USA

C. Huber
School of Earth and Atmospheric Sciences,
Georgia Institute of Technology, Atlanta, GA 30332, USA

A. Skopelitis
Section des Sciences de la Terre et de l'Environnement,
Université de Genève, Rue des Maraîchers 13,
1205 Geneva, Switzerland

C. Schnyder
Muséum d'Histoire Naturelle de Genève,
1 route de Malagnou, 1208 Geneva, Switzerland

Published online: 29 June 2011

Introduction

The Kos-Nisyros Volcanic center (KNVC) is a Plio-Pleistocene magmatic system located on the eastern edge of the Aegean subduction zone. Over the last 3–4 million years, it produced a wide variety of magma compositions (from basaltic andesite to high-SiO_2 rhyolite; see Francalanci et al. 2007 for a compilation), as is typical of a long-lived volcanic center in subduction zones. Its eruptive history culminated in a large caldera-forming event 161 ka ago: the Kos Plateau Tuff (KPT). This >60 km^3, high-SiO_2, crystal-rich unit is an important turning point in the evolution of silicic magmas in the area. Before and during evacuation from their shallow magmatic hearth, the rhyolitic magmas were low temperature (<750°C), oxidized (~NNO+ 1), and contained low-temperature minerals (biotite-quartz-sanidine). Immediately after the KPT eruption, basalts and andesites were the first magmas to reach the surface along the southern edge of the KPT caldera. Silicic compositions reappeared only after an incubation time of several tens of thousands of years. The first of these evolved magmas has obvious differences with the caldera-forming unit and its immediate predecessors: they contain a completely different mineral assemblage and are slightly more mafic (rhyodacites instead of high-SiO_2 rhyolites). However, in the most recent eruptions, the magmas have returned to high-SiO_2 rhyolites similar to those observed prior to and during the caldera collapse. This paper focuses on explaining this abrupt petrologic change after the caldera collapse and the progressive recovery that ensued.

Settings

The Kos-Nisyros Volcanic Center (KNVC) is located on the eastern edge of the Aegean Sea (Fig. 1). It is the easternmost volcanic system of the active South Aegean arc, which results from the subduction of the African plate underneath the Aegean microplate at a rate of <1 cm/year (Jackson 1993; Wortel and Spakman 2000). It is built on Paleozoic–Mesozoic basement rocks (Alpine basement) that were deformed during the Tertiary by the Hellenide orogeny (Pe-Piper and Piper 2002). The Kos-Nisyros volcanic center has been active for at least 3 million years (Bachmann et al. 2010) and continues to show signs of unrest (Papadopoulos et al. 1998; Caliro et al. 2005; Gottsmann et al. 2005; Lagios et al. 2005; Pe-Piper et al. 2005).

Calc-alkaline Pliocene volcanism in the area started on the western peninsula of the Island of Kos (Kefalos Peninsula), with the oldest dated rocks exposed as dacitic domes (Matsuda et al. 1999; Bachmann et al. 2010). It is, however, likely that andesitic units, now only preserved as

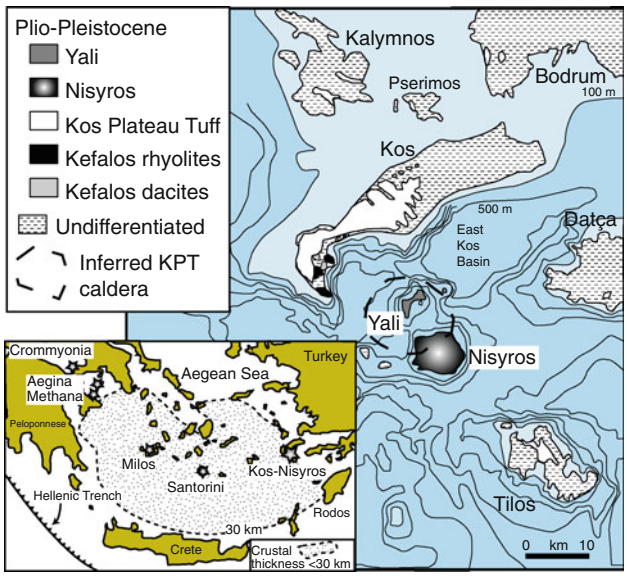

Fig. 1 Location map of the Kos-Nisyros volcanic center (modified from Pe-Piper et al. 2005; Bachmann 2010)

lithic clasts in the KPT and small islands to the west of Nisyros Island (Pachia and Pyrgoussa), erupted prior to 3 Ma. Multiple rhyolite domes and pyroclastic flows also were emplaced in the Kefalos area (Cheri-Agios Mammas, Latra, Karanas, Zini, Kefalos Series; Dabalakis and Vougioukalakis 1993; Pe-Piper and Moulton 2008). These rhyolites all appear to be younger than 3 Ma, but dating remains imprecise. Available K–Ar data (Bellon and Jarrige 1979; Pasteels et al. 1986) range from 2.7 to 0.23 Ma, but most likely suffer from some excess ^{40}Ar (Bachmann et al. 2010), yielding unreliably older eruption ages. Single zircon U/Pb TIMS analyses on a couple of domes (Agios Mammas and Zini) and Kefalos Series pyroclasts have also been performed and suggest eruption ages around 0.3–0.5 Ma (Bachmann et al. 2010).

At 161 ka, the largest recorded eruption of the KNVC, the Kos Plateau Tuff, occurred from a stratovolcano located between the islands of Kos and Nisyros (present location of Yali Island); it evacuated >60 km^3 of ash and pumice in the atmosphere and blanketed the neighboring lands with a thick nonwelded ignimbrite (Allen 2001). The presence of abundant sanidine in the deposits permitted a precise determination of its eruption age (161 ± 1 ka; Smith et al. 1996, 2000), while abundant zircons show that the magma body had been growing over >200 ky (Bachmann et al. 2007).

After the KPT eruption, the locus of volcanism shifted south to the present islands of Nisyros and Yali (and the tiny islet of Strongili), which have been entirely constructed over the last 160 ky (Pe-Piper and Moulton 2008). Dating of Nisyros and Yali units has proved extremely challenging as (1) there are no K-bearing phases (no

accurate K–Ar or Ar–Ar ages for these young units) and (2) rocks are either too old for ^{14}C or did not preserve measurable amounts of C (Volentik et al. 2006). Other techniques have been applied (fission tracks on volcanic glass, calibration with oxygen-isotope stratigraphy of extrapolation based on sedimentation rate) with limited success (Volentik et al. 2006; Bachmann et al. 2010). However, stratigraphic packages still allow one to elucidate a general magmatic evolution of Nisyros (Vanderkluysen et al. 2006b). Volcanism started with basaltic andesite lavas (mostly preserved as pillow lavas on the northwest side of the volcano) and gradually built a subaerial cone with more evolved lavas. The last large eruptions on Nisyros were rhyodacitic to rhyolitic (Lower Pumice, Nikia lava flow, and Upper Pumice, which has a ^{14}C age of 42–44 ka; Aksu et al. 2008). All three eruptions involved a few km^3 of magma (Limburg and Varekamp 1991; Vanderkluysen et al. 2006b; Longchamp et al. 2011).

The youngest sizeable deposits of the Kos-Nisyros Volcanic Center form the Island of Yali. It is dominantly rhyolitic and consists of both explosive and effusive deposits, with a submarine pumice cone (Allen and McPhie 2000) and obsidian lava flows sharing the exposures on the island. Other than a fission track age of 24 ka on volcanic glass (Wagner et al. 1976), the only reliable ages on Yali deposits come from marine tephrochronology (Aksu et al. 2008), which yield an approximate age between 39 and 22 ka. However, stratigraphic relationships (fine pumice layer within the Nisyros caldera) suggest that the Yali pumice erupted after the Lower and Upper Pumice on Nisyros.

This paper focuses on the evolution of silicic magmas of Kos-Nisyros-Yali (dacites and rhyolites; Fig. 2) during the entire lifetime of the system. We consider the dacitic-rhyolitic units on Kefalos (Vigla and Kastelli dacites, Mount Latra, Zini, Agios Mammas and Kefalos Series Pyroclasts), the Kos Plateau Tuff, as well as the rhyodacites to rhyolites erupted on Nisyros and Yali (Lower and Upper Pumices, Nikia lava flow, Yali Pumice). These units, and more mafic deposits on Nisyros, have been discussed previously by others (e.g., Di Paola 1974; Wyers and Barton 1989; Limburg and Varekamp 1991; Francalanci et al. 1995; Buettner et al. 2005; Vanderkluysen et al. 2006a; Francalanci et al. 2007; Zellmer and Turner 2007; Pe-Piper and Moulton 2008), but have never been looked at as a continuous eruption sequence with consideration of the consequent implications for magma evolution.

Analytical methods

Representative samples from all silicic units mentioned in the above paragraph were collected in areas free of any visible alteration. For Yali samples, all analysed material comes from fresh pumice blocks gathered near the top of the submarine pumice cone. Whole-rock analyses by XRF, mineral chemistry by electron microprobe, trace element concentrations in zircons by SHRIMP, and Hf isotopes in zircons by laser ablation and solution MC-ICP-MS were acquired using methods fully described in a data repository file (Appendix 1). Whole-rock analyses by XRF are fully consistent with previously published analyses of the same units.

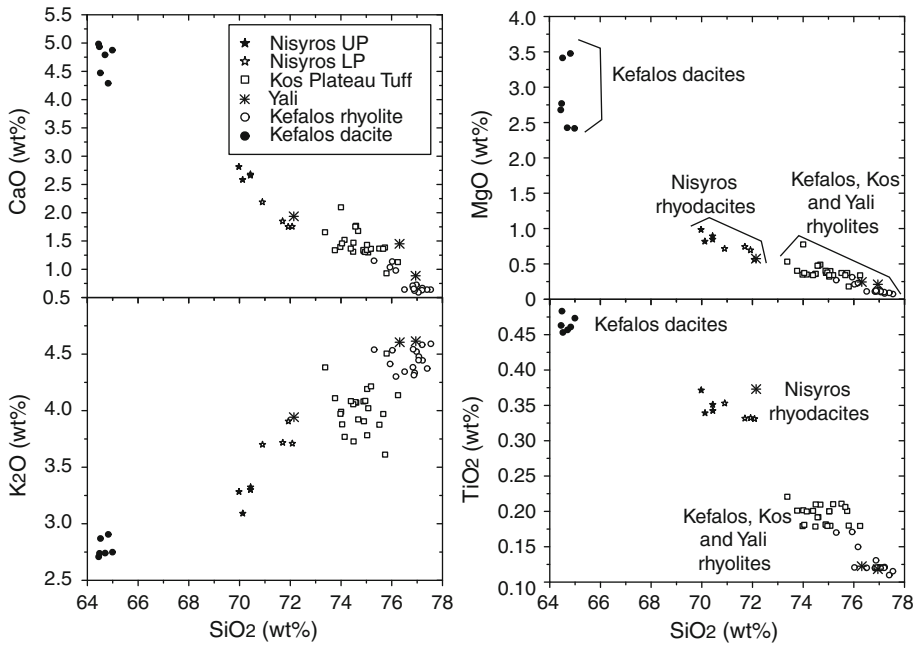

Fig. 2 Major element compositions of selected silicic volcanic units from the Kos-Nisyros volcanic centers

Results

Whole-rock compositions

Whole-rock compositions vary from 64–65 wt% SiO_2 (Kefalos dacites) to 69–72 wt% SiO_2 for the Nisyros units (Lower Pumice, Nikia, Upper Pumice) and 73–76 wt% SiO_2 (Kefalos rhyolites, KPT, Yali rhyolites; the less silicic being mixed pumices in the KPT and Yali; Allen and McPhie 2000; Bachmann 2010; Fig. 2). There is a >4 wt% SiO_2 compositional gap between the dacites and the rhyodacites. This gap is evident for many major and trace elements (Figs. 2, 3, 4, and 5). Trends in major and trace element concentrations (particularly in Ba, Y, Sr, and Zr) display a liquid line of descent (LLD) that markedly differs from other evolved rhyodacites to rhyolites, such as those found in the Long Valley area (Bishop Tuff; Hildreth and Wilson 2007), and particularly from the Yellowstone area (e.g., Bindeman and Valley 2001). These obvious differences in trace element concentrations indicate variations in the abundance of the major crystallizing phases (typical arc LLD with less plagioclase and pyroxene, but more abundant amphiboles and oxides in the case of the Aegean rocks in comparison to Yellowstone; see following sections). For example, Sr is much higher (and Nb much lower) in KNVC units compared with Yellowstone magmas, indicating delayed plagioclase crystallization and a higher involvement of oxide minerals in the case of the KNVC magmas.

Among the KNVC units, the Nisyros units have slightly higher Y and Zr than both the Kefalos dacites and the high-SiO_2 rhyolites of Kefalos and KPT (Fig. 4). Higher Zr contents in Nisyros units translate into a higher zircon saturation temperature. These trends suggest that the Nisyros rhyodacites evolved from intermediate magmas with less amphibole and zircon than that experienced by the Kefalos and KPT rhyolites (see also Buettner et al. 2005). The Nisyros intermediate magmas that evolved to the rhyodacites were also hotter (above zircon saturation temperature; see also thermometry results below). The Yali rhyolite has Zr contents similar to the Kefalos-KPT rhyolites, but Y contents comparable to the Nisyros units, confirming its transitional character.

Mineralogy and mineral chemistry

Mineral assemblage

The mineralogy of erupted silicic magmas varied markedly over the lifetime of the KNVC (Table 1). In the sequence of units we discuss in this paper, dacites were the first to erupt on Kos island (Kefalos peninsula; Trapezina and Vigla dacites; Pe-Piper and Moulton 2008). They are crystal-rich (40–50% crystals) and are characterized by an assemblage of plagioclase, amphibole, biotite, and Fe–Ti oxides. Following these dacites, rhyolites erupted, first as small volumes on the Kefalos Peninsula (both domes and pyroclastic flows), then as a large volume ignimbrite (KPT) in the basin south of Kos Island where the caldera is located. Kefalos rhyolites are crystal-poor (with 2–5 vol% crystals), while the KPT is crystal-rich (30–40 vol%

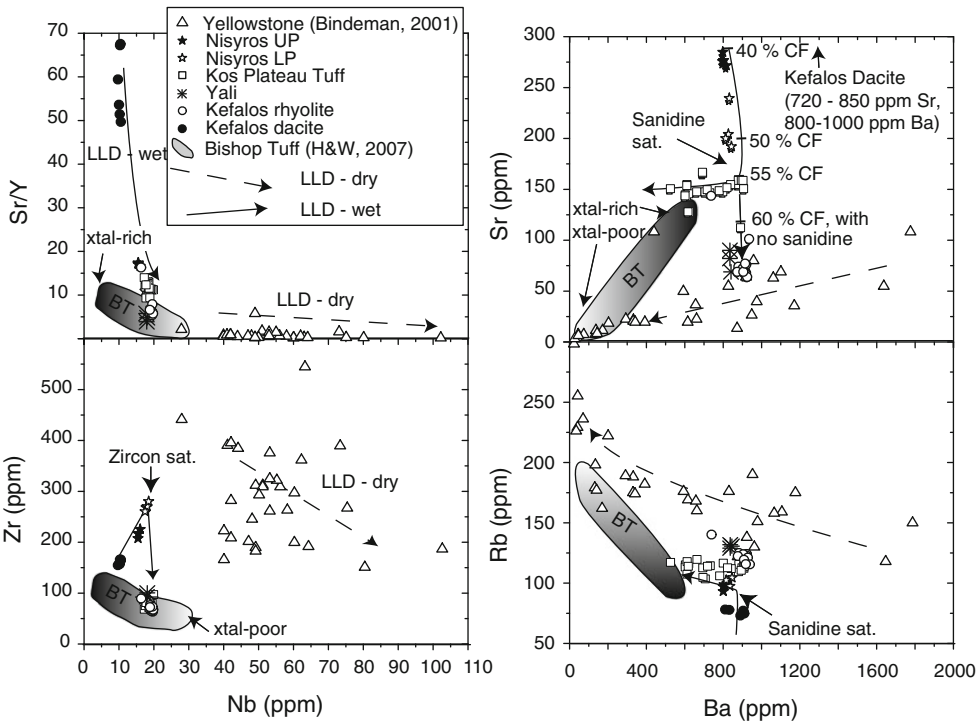

Fig. 3 Selected trace element concentrations in silicic volcanic units of the Kos-Nisyros volcanic center, in comparison to other well-studied silicic units in different tectonic settings (Yellowstone and Bishop Tuff (*BT*)). On the Ba-Sr diagram, Rayleigh crystal fractionation modeling shows that the rhyolites were produced by 50–70% crystallization of the Kefalos dacite using the phase assemblage observed in the dacite (plag, hbl, oxides, leading to a bulk D_{Sr} of ~5 and a bulk D_{Ba} of ~1). The change in crystal concentration from the early crystal-poor to the late crystal-rich Bishop Tuff (*BT*) is portrayed by the grayscale gradient

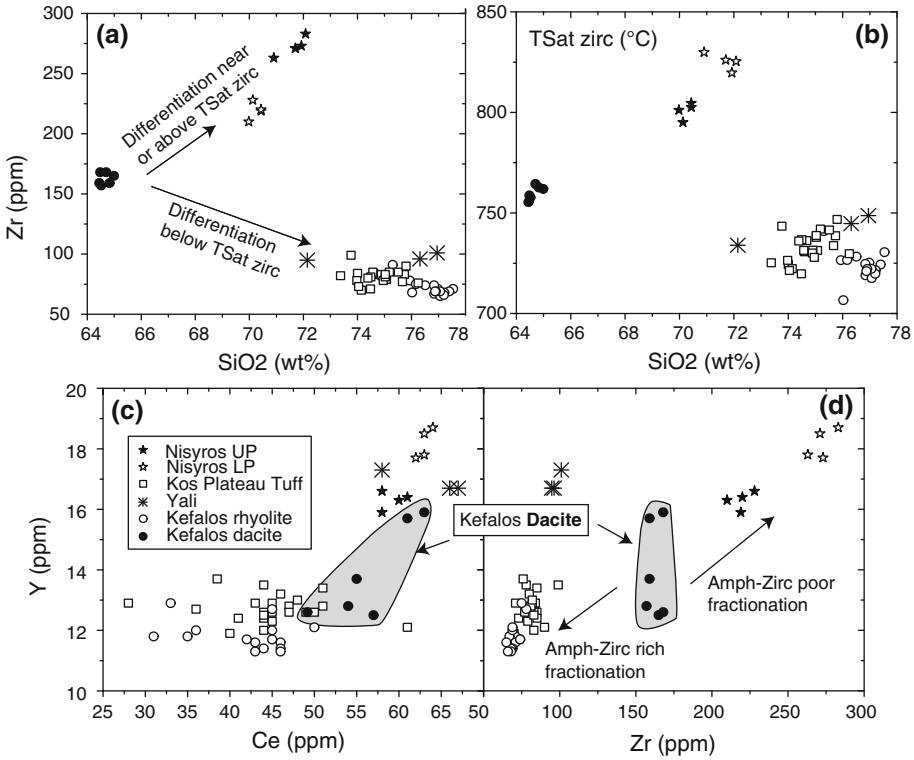

Fig. 4 **a** Zr content and **b** zircon saturation temperature ("TSat zirc", using whole-rock Zr content; Watson and Harrison 1983) for the Kos-Nisyros volcanic center, showing differentiation from a hot, zircon-poor mush for the case of Nisyros, and a cold, zircon-bearing mush for the case of Kefalos-KPT-Yali. *Lower* Y in Kefalos-KPT rhyolites (**c** and **d**) also indicates lower amphibole involvement. Note that high-Y high-Zr rocks do not exist (basalts-andesites typically show high Y but low Zr). Amph stands for amphibole and zirc for zircon

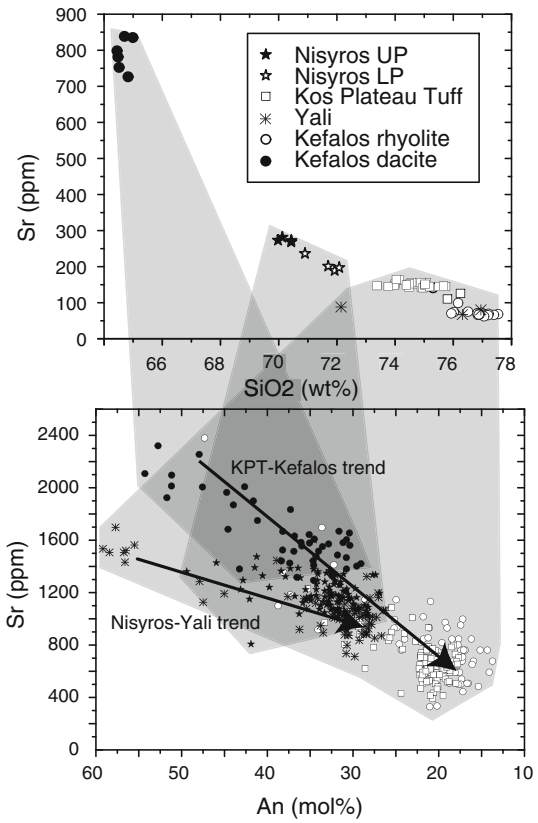

Fig. 5 Sr variations in whole-rock and plagioclase phenocrysts, showing significant overlap between the dacites and the rhyolites

crystals). They share a similar mineral assemblage, consisting of plagioclase, biotite, quartz, and oxides, but the KPT also contains sanidine, often complexly intergrown with plagioclase (Rapakivi texture, Bachmann 2010). In contrast, the next silicic units to erupt in the KNVC (on Nisyros Island, after an interval dominated by more mafic magmas) are rhyodacitic, do not show any biotite, quartz, or sanidine (except Profitis Ilias, which has rare quartz), have very little amphibole, but display abundant pyroxene (both clino and orthopyroxene) and plagioclase. The latest silicic eruptive products (Yali rhyolite, both explosive and effusive) breached the surface from vents halfway in between Kos and Nisyros, perhaps sitting on or near the northern end of the KPT caldera (Pe-Piper and Moulton 2008). These Yali units display petrological characteristics of both Kos and Nisyros; in addition to plagioclase and oxides, which are in all studied units, Yali deposits contain pyroxene (although out of equilibrium with its melt; see Appendix 2), but also contain biotite, hornblende, quartz, and sanidine.

Mineral chemistry

Plagioclase

Plagioclase compositions, despite the chemical zonation that is common in evolved arc rocks, generally reflect their

Table 1 Mineral assemblages present in the different silicic volcanic units

	Kos Island			Nisyros Island						Yali
	Kefalos Dacite	Kefalos rhyolites	KPT	Avlaki	Emborio lava	LP	Nikia	UP	Trapezina	Profitis Elias	Yali pumice
SiO_2 content (wt%)	64–65	75–77	74–76	69–70	~66	69–72	70–72	68–70	67–68	67–68	75–76
Age (ka)	~3,000	~2,500–500	160	n.d.	n.d.	n.d.	n.d.	>40	<40	n.d.	~30–20
Crystal content (vol%)	40–50	2–5	30–40	~5–15	~20–25	~7–10	~20–30	15–20	n.d.	~20–40	~5–8
Pl	■	■	■	■	■	■	■	■	■	■	■
Am	■			•	•	•	•	•	•	•	•
Px				■	■	■	■	■	■	■	•
Qtz		•	■							•	•
Bt	•	•	•								•
Sn			■								•
Ox	•	•	•	•	•	•	•	•	•	•	•
Ap	•	•	•	•	•	•	•	•	•	•	•
Zrc	n.d.	•	•	n.d.	n.d.	•	•	•	n.d.	n.d.	•

Ages for Nisyros are poorly constrained and most units have not been dated. See Bachmann et al. 2010 for reference

Large symbols indicate an abundant phase, while small symbols indicate a minor phase

n.d. not determined

whole-rock compositions ($An_{55–30}$ in Kefalos dacites, $An_{50–30}$ in Nisyros rhyodacites, and $An_{50–15}$ in Kos and Yali rhyolites; Fig. 5; Bachmann 2010). Interestingly, while the whole-rock chemical data show a 4–5 wt% SiO_2 gap between the dacites and the rhyodacites, the plagioclase compositions overlap extensively (Fig. 5). They also show a clear progressive crystal fractionation trend from high An—high Sr to a low An—low Sr content. There are subtly different trends in Sr-An, with Nisyros compositions having a lower Sr for a given An content (above $\sim An_{40}$). Using the latest calibration of the plagioclase–liquid hygrometer (Lange 2009), values for Nisyros rhyodacites cluster around 4.5–5 wt% H_2O (at ~850°C and 2.5 kb). Such estimates have not been attempted for the KPT and Yali as their compositions are too silicic for Lange (2009) plagioclase hygrometer's calibration.

Pyroxene

Both clino and orthopyroxene (CPX and OPX) compositions are fairly homogeneous in Nisyros units (Appendix 2); their Mg# (mole % Mg/(Mg + Fe)) clusters between 70 and 75 for CPX and 55–65 for OPX. On the other hand, those pyroxenes found in Yali units are clearly highly variable and out of equilibrium with the coexisting melt (Appendix 2). The Yali CPXs are strongly zoned (low Mg rim and high Mg core; Appendix 3) and the OPXs are resorbed (Appendix 3). All compositions found in Yali are too Mg-rich to be in equilibrium with a rhyolitic melt (using Putirka 2008 test for cpx-melt equilibrium).

Amphibole

In the Kefalos dacites, amphiboles have highly variable compositions and are strongly zoned (Appendix 4a and b). They range from tschermakitic pargasite to Mg-hornblende (using the classification of Leake et al. 1997), with Al_2O_3 from 12.5 to 6.5 wt% (corresponding to Al# = $^{vi}Al/^{iv}Al$ from >0.25 to close to 0, although they mostly cluster <0.1). Several hornblende crystals display rimward enrichment in Al_2O_3 (see example in Appendix 4b). Amphibole phenocrysts in other units (Nisyros and Yali) are rare, smaller, and show a more restricted range in compositions. They mostly vary from 10 to 7 wt% Al_2O_3; only a couple of analyses from crystals in Yali pumice are as low as 5.5 wt% Al_2O_3.

Biotite

Biotite crystals, when present (only in Kefalos, Kos, and Yali units), are euhedral and chemically homogeneous. KPT biotite crystals have proven very difficult to analyze by electron microprobe (>90% of analyses give oxide

totals that are lower than 95%). Detailed TEM work seems to indicate the potential presence of saline fluid inclusions in these KPT biotite crystals (Bachmann 2010). However, the biotite crystals in Kefalos units do not show such characteristics and provide reliable analyses by electron microprobe (Bachmann et al. 2010). When compared to KPT biotites with acceptable total oxides (95–97%), the Kefalos biotites are generally similar; they have typical compositions for such silicic compositions (37–38 wt% SiO_2; 8.5–8.8 wt% K_2O; 13.6–14.7 wt% MgO; Bachmann et al. 2010).

Fe–Ti oxides

Magnetite and ilmenite crystals are found in all units in small quantities (trace to 1–2 modal %). They are strongly exsolved in the domes on the Kefalos Peninsula (both in the dacites and rhyolites). However, rapidly-cooled pyroclastic units on Kefalos, Kos, Nisyros, and Yali provide oxide pairs that are, in most cases, in Mn–Mg equilibrium (Bacon and Hirschmann 1988). Temperature and f_{O_2} determinations using these pairs are reported in the section below.

Zircon

Zircon crystals are present in all of the units that were examined for their presence (Kefalos rhyolites, KPT, Nisyros UP and LP, Nikia flow, Yali Pumice) and are most likely also part of the mineral assemblage in the other rhyodacites to rhyolites (listed as not determined, n.d., in Table 1). On the basis of the fairly low Zr concentration in the Kefalos dacite ($\sim$160 ppm), zircon would have been saturated only at a low temperature (zircon saturation temperature is $\sim$760°C) and are most likely not very abundant.

Zircons are reliable recorders of magmatic conditions in which they grow because of their resistance to chemical resetting at magmatic conditions and their ubiquitous presence in silicic magmas. We used zircons extracted from the rhyolites (Kefalos—KPT—Yali) and from the rhyodacites (Nisyros) to complement the whole-rock geochemical data and to determine magma storage conditions for both rhyolites and rhyodacites (see Appendix 1 for analytical techniques).

All analyzed zircon crystals in the KNVC are chemically zoned, showing significant variations in minor and trace elements (Appendix 5). However, the range of variations they display is very similar among the different units (apart from Kefalos zircons, which show some outlying compositions, most likely a consequence of the higher proportion of inherited crystals in these Kefalos units compared with KPT; see "Discussion" and Bachmann et al. 2010). The main difference between Nisyros-Yali and KPT zircons is their concentrations in some trace elements, including Ti, Hf, U, Sc, and Nb (Figs. 6 and 7, Appendix 5 and 6). The lower Ti content of KPT zircons reflects a lower crystallization temperature (e.g., Fu et al. 2008), while the typically higher Hf, U, Sc, and Nb contents reflect the slightly more evolved melt composition from which these zircons crystallized. We also note some high Ce-Y-Yb and low Hf cores, mostly in the KPT zircons. As Hf in zircon is considered to be a reliable indicator of melt evolution (Claiborne et al. 2006), these cores are likely early-crystallized parts of the crystals, formed immediately after a recharge event by a more primitive magma.

The spread in trace element compositions we observe in KNVC zircons is similar to that seen in silicic plutonic magmas from the Spirit Mountain Batholith (Fig. 5 and 6; Claiborne et al. 2010) and the Tatoosh Intrusive Suite (du Bray et al. 2010). Both plutonic suites contain zircons that encompass fairly early (Nisyros-type) and rather late, evolved (high Hf, Yali, KPT) zircons. This indicates that volcanic and plutonic zircons, at least in these systems, are evolving in very similar conditions.

Apart from zircons from the Kefalos rhyolites, Hf isotope ratios of zircon crystals from KPT, Nisyros, and Yali yield similar ranges. The εHf values determined by LA-MC-ICPMS on zircons (Table 2; Fig. 8; Appendix 7) are in good agreement with previously published whole-rock

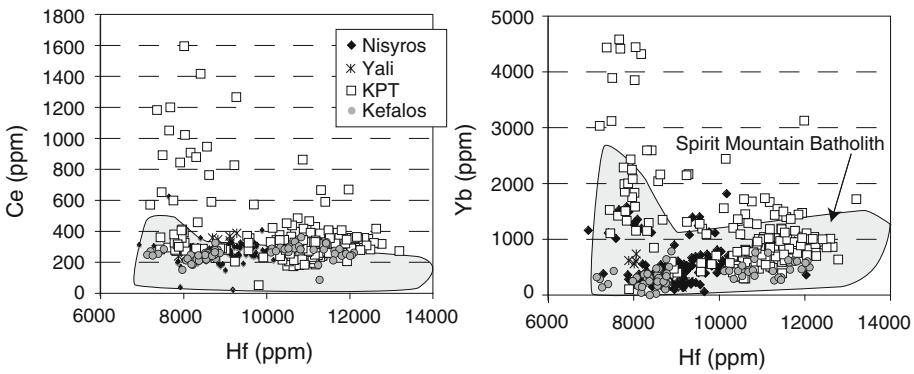

Fig. 6 Electron microprobe data for zircons from Kefalos, KPT, Nisyros (including Nikia flow), and Yali units. Data for the Spirit Mountain Batholith are from Claiborne et al. 2010)

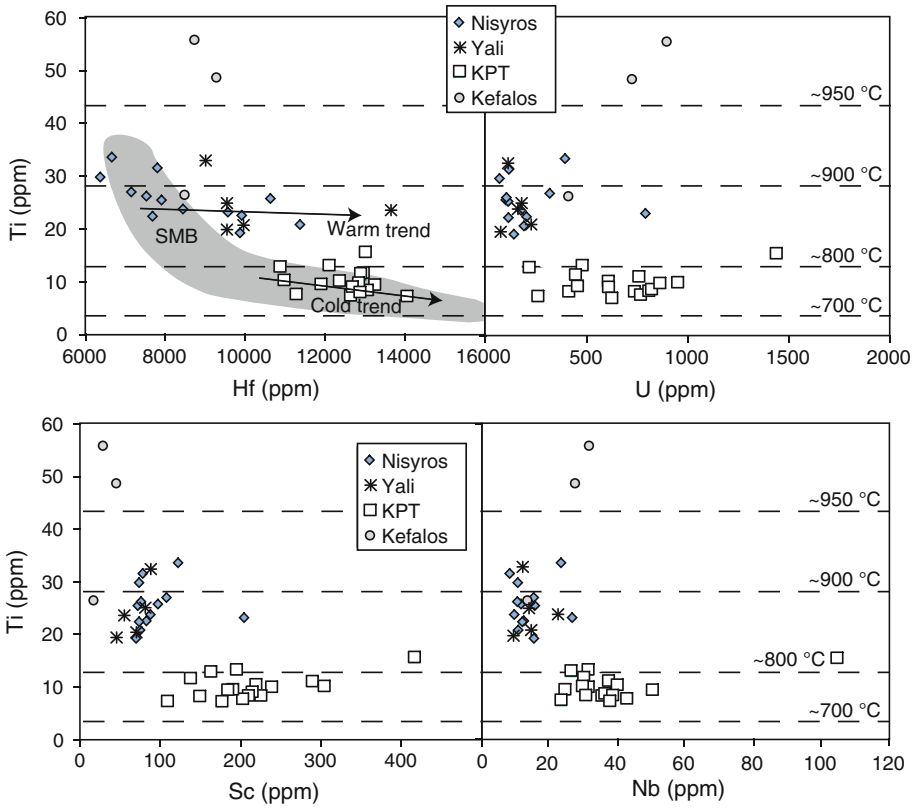

Fig. 7 Selected trace element concentrations in Kefalos, KPT, Nisyros, and Yali zircons measured by SHRIMP. *Shaded region* in data shows Ti vs. Hf from the Spirit Mountain Batholith (SMB; Claiborne et al. 2010)

Table 2 Average εHf values of zircons by in situ LA-MC-ICPM

Sample	Number of spots	εHf	±	Description
KPT04–7	8	2.46	2.83	KPT pumice
KPT04–24	24	1.96	2.24	KPT pumice
KPT04–21	5	4.76	3.55	KPT pumice
KPT04–28	5	3.24	3.38	KPT pumice
KPT04–36	7	5.15	2.18	KPT pumice
KPT Pum1	6	5.32	3.19	KPT pumice
KPT04–15	4	4.85	3.02	KPT granitic enclave
KPT04–20	4	3.86	3.21	KPT granitic enclave
KPT04–37	5	3.32	3.57	KPT granitic enclave
KPT Xeno4	9	4.87	3.10	KPT granitic enclave
Nis 1	4	4.12	1.40	Nisyros UP pumice
Nis UP	5	3.72	2.13	Nisyros UP pumice
Nis UP05	10	4.52	1.97	Nisyros UP pumice
Nikia	11	4.25	1.80	Nikia lava flow
Yali	7	4.62	2.32	Yali pumice
KS06–7	11	−1.83	1.43	Kefalos Series pumice
KS06–19	7	−0.14	1.30	Kefalos Series pumice
KS06–23	9	−2.93	1.15	Kefalos Series pumice

A complete data table with all laser ablation spots, bulk zircon digestions, and whole-rock values is given in "Appendix 1"

These averages were calculated only from analyses that had undergone an interference correction of <40%

data on three of the same units (Nisyros UP, Nikia lava flow, Yali rhyolite; Buettner et al. 2005) and bulk zircon dissolution analyzed by standard solution MC-ICPMS. The εHf generally falls between 0 and +10, in accord with relatively mantle-like Sr ($^{87}Sr/^{86}Sr \sim 0.704$–$0.7045$) and Nd ratios ($\varepsilon Nd \sim -2$ to +3; Bachmann et al. 2007; Zellmer and Turner 2007; Pe-Piper and Moulton 2008; Bachmann 2010) on Kos and Nisyros whole-rock samples.

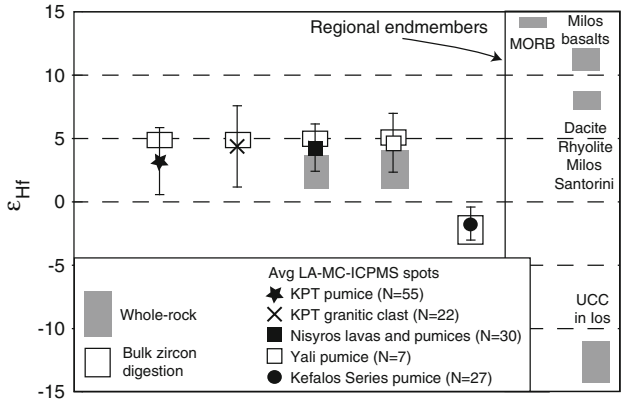

Fig. 8 Average εHf data from laser ablation and solution MC-ICPMS data on zircons from the Kos-Nisyros volcanic center and regional whole-rock values from Briqueu et al. 1986; Milos, Santorini) and Buettner et al. 2005; MORB, UCC, Ios, and Nisyros-Yali units). UCC refers to Upper Continental Crust in the region. The local UCC was sampled as gneisses on Ios (Buettner et al. 2005)

Only zircons from Kefalos Series rhyolite show, on average, negative εHf values, suggesting a greater crustal contribution. The observed range of εHf values in the KNVC rhyolites is corroborated by zircon U–Pb dating (both CA-TIMS and SHRIMP) in the area, which show no zircon inheritance for the KPT, but significant zircon inherited from the crust for the Kefalos rhyolites (with single zircon U/Pb ages up to 20 Ma; Bachmann et al. 2007; Bachmann et al. 2010).

P–T-f_{O_2} conditions of crystallization

As oxides are present in all KNVC units, Fe–Ti oxide thermometry can be applied to most units, except in Kefalos dacites, where ilmenites and magnetites show fine-scale exsolution lamellae, suggesting reequilibration at the surface. In all other cases, pairs of oxides in Mg–Mn equilibrium (Bacon and Hirschmann 1988) have been analyzed by electron microprobe at the University of Lausanne to calculate temperature and oxygen fugacities, using the latest calibration for T-f_{O_2} models (Ghiorso and Evans 2008). As a comparison to these T-f_{O_2} estimates, we also used two-pyroxene thermometry (using the QUILF software) on Nisyros units (where pyroxene appears to be in equilibrium), the thermo-barometric calculations of Ridolfi et al. (2010) using amphiboles and the amphibole-plagioclase thermometer of Holland and Blundy 1994 on amphibole-bearing units (Kefalos dacite, Nisyros and Yali).

For the Kefalos rhyolites and KPT, Fe–Ti oxide pairs in Mn–Mg equilibrium yield very low temperatures (using Ghiorso and Evans 2008 calibration), clustering around 680–700°C (with an f_{O_2} of NNO +0.5 to 1; Fig. 9b). Fe–Ti oxide temperatures are significantly higher (and oxygen fugacities slightly lower) for Nisyros, yielding temperatures between 800 and 850°C (and NNO to NNO +0.5; Fig. 9b). As only a few of the analyzed oxides in Yali units were in equilibrium, temperatures and oxygen fugacities determined using oxide pairs are not reliable.

A preeruption temperature estimate for the KPT magma of ~700°C is supported by the presence of low-temperature phases in this wet magma (sanidine and quartz), as well as by similar temperatures obtained using two-feldspar thermometry and Ti-in-quartz thermometry (Bachmann 2010). Similarly, higher temperatures of 800–850°C for Nisyros units were also obtained using two-pyroxene thermometry. Using QUILF (Andersen et al. 1993), pyroxene temperatures vary from 815 to 915°C, with an average around 850°C. As pyroxenes are either strongly zoned or resorbed in Yali, they were not used to determine temperatures in this unit.

The range in temperature estimates using amphibole (e.g., Ridolfi et al. 2010) and amphibole-plagioclase (thermometer B of Holland and Blundy 1994) is large for the Kefalos dacite (from 700 to 850°C for the Holland and Blundy 1994 calibration at 2 kb—An37 plag, and from 750 to 950°C using Ridolfi et al. 2010 calibration), with averages around 775°C for Holland and Blundy (1994) and 875°C for Ridolfi et al. (2010; Fig. 10). Amphiboles in Nisyros and Yali units are not as strongly zoned, but still display a significant range in temperature,

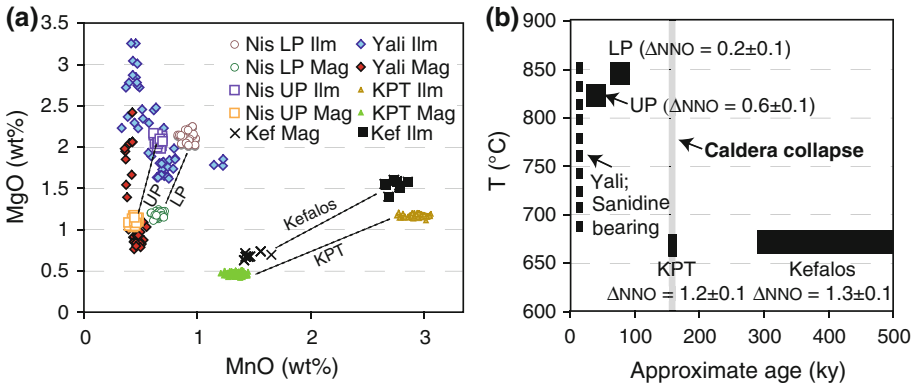

Fig. 9 **a** MnO and MgO contents of Fe–Ti oxides in Kefalos, KPT, Nisyros, and Yali units (UP stands for Upper Pumice and LP for Lower Pumice; both erupted from Nisyros). **b** T and f_{O_2} based on the model of Ghiorso and Evans (2008) for the same units (all pairs in Mn–Mg equilibrium. Note the remarkable change in T and ΔNNO after the caldera collapse

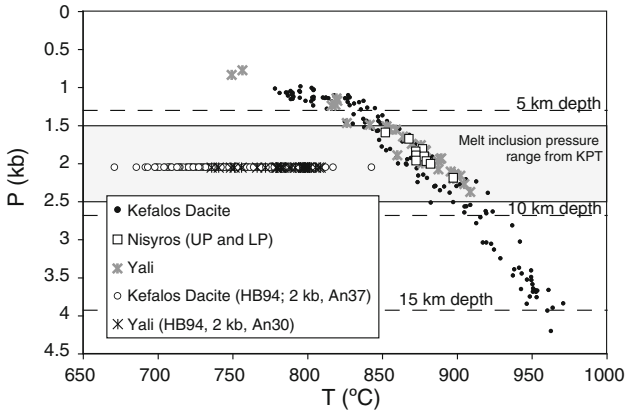

Fig. 10 Estimates of P and T from Ridolfi et al. (2010). For comparison, temperatures from Holland and Blundy 1994 Thermometer B at 2 kb at also shown. HB94 is Holland and Blundy 1994, and An37-An30 are the anorthite concentrations of plagioclase crystals in equilibrium with hornblende compositions. Gray field is the pressure yielded by quartz-hosted melt inclusions in the KPT (Bachmann et al. 2009)

from 720 to 800°C for the Holland and Blundy 1994 calibration (at 2 kb—An_{30} plag) and from 750 to almost 900°C using the Ridolfi et al. 2010 calibration.

Pressures of crystallization, H_2O content, and f_{O_2} can also be recovered using amphibole chemistry and the Ridolfi et al. 2010 calibration. Pressure estimates for the Kefalos dacite range from nearly 4.5–0.75 kb (from 15 to 3 km depth), while Nisyros and Yali units are clustered between 1 and 2.50 kb (10 to 4 km depth). This range is similar to that found for the KPT using melt inclusion data (Bachmann et al. 2009), albeit slightly shifted toward lower pressures. Based on the results presented in Fig. 10, we suspect that the Ridolfi et al. 2010 calibration overestimates temperatures and underestimates pressures for the low-Al amphiboles found in very silicic magmas. Oxygen fugacity varies from NNO +0.5 to NNO + 1 for Nisyros units, and up to NNO + 1.7 for some analyses of Yali amphiboles. These values are on average slightly higher than those obtained by Fe–Ti oxides (Ghiorso and Evans 2008 calibration between NNO +0.2 to 0.6 for Nisyros and up to NNO +1.3 for KPT and Kefalos; Fig. 9b). Water contents for these magmas cluster around 4.5 to 5.5 wt% H_2O, on average slightly lower than quartz-hosted melt inclusion data in the KPT (Bachmann et al. 2009).

Discussion

Origin of the magmatic diversity in the KNVC

Most commonly, magmatic diversity in the KNVC has been attributed to fractional crystallization of a wet liquid line of descent (with abundant amphibole) associated with some crustal assimilation (AFC; Di Paola 1974; Wyers and Barton 1989; Francalanci et al. 1995; Buettner et al. 2005; Bachmann et al. 2007; Zellmer and Turner 2007; Pe-Piper and Moulton 2008; Bachmann 2010). Our new Hf isotope analyses on zircons (both multi-grain dissolution and LA-MC-ICPMS; Fig. 8) corroborate this claim, as they show average εHf around +5 for both KPT and Nisyros units (despite significant ranges observed in the laser ablation data, suggesting some zoning in Hf isotope ratios). Along with whole-rock Sr, O, He, Hf, and Nd isotope ratios (Buettner et al. 2005; Shimizu et al. 2005; Bachmann et al. 2007; Zellmer and Turner 2007; Pe-Piper and Moulton 2008), these in situ Hf isotope analyses in zircon suggest a significant component of mantle-derived material in these magmas, as local basalts yield whole-rock εHf values between +10 and +13 (Briqueu et al. 1986). The Kefalos rhyolites yield less radiogenic εHf (averages between 0 and −5), indicating a larger crustal contribution in its zircon population. CA-TIMS dating of individual Kefalos rhyolite zircons supports this inference as it shows a significant fraction of xenocrystic zircons, with ages up to 20 Ma (Bachmann et al. 2010).

Precisely determining the proportions of different reservoirs (slab, sediments, mantle wedge, lower crust, upper crust) in forming magmas using radiogenic (and stable) isotopes has proven extremely difficult in the Kos-Nisyros area (and in the Aegean region in general; Briqueu et al. 1986; Pe-Piper and Piper 2002; Buettner et al. 2005; Shimizu et al. 2005; Zellmer and Turner 2007; Pe-Piper and Moulton 2008). Although radiogenic isotopes in KNVC magmas all show some component of old continental crust, how much was added and the identity of the reservoirs involved remains unclear. The actual isotope ratios for individual reservoirs are generally poorly defined, and the different isotope systems appear decoupled (mantle extraction ages are ~850 Ma for Nd, ~750 Ma for Hf, and only 50–100 Ma for Sr; Buettner et al. 2005). On the basis of the complex sedimentary pile being subducted into the Aegean trench (thick Nile sediments), the thin continental crust of the Aegean microplate (not conducive to large amounts of assimilation; Dufek and Bergantz 2005) and the potential involvement of primitive fluids (Buettner et al. 2005) and lithospheric mantle in the source zone (Mitropoulos and Tarney 1992), we believe it is likely that much of the substantial isotope heterogeneity was inherited from the mantle source, although an unambiguous test of such an inference is unforeseen at present.

In order to illustrate plausible amounts of assimilation, assimilation-fractional crystallization (AFC) models (DePaolo 1981) were run using carefully constrained trace element concentrations, reservoirs' isotope ratios, and bulk partition coefficients (see caption of Appendix 8 for values). These models show that, for these conditions, KNVC

silicic magmas are best explained by 80–90% crystallization, assuming an r value of ~ 0.1 (r = assimilation rate/crystallization rate; DePaolo 1981). As the calculations assumed an initial basaltic composition, 80–90% crystallization is required to reach rhyolite to rhyodacite composition. Moreover, as the crust is thin, an r value larger than ~ 0.1 seems unlikely based on thermal models. This r value is an average over the course of differentiation and could have been higher in the lower crust and correspondingly lower in the upper crust. In summary, these models provide geologically sound, albeit basic, AFC evolution patterns for the KNVC magmas.

In the AFC framework, magma evolution in the KNVC sequence is envisioned to follow a polybaric path that first requires generation and extraction of intermediate magmas from the lower- to mid-crust, followed by storage and reservoir growth in the upper crust—similar to models developed for other large, silicic systems (not discussed in detail in this paper, but see for example Mann 1983; Hildreth and Moorbath 1988; Wyers and Barton 1989; Riciputi et al. 1995; Dufek and Bergantz 2005; Annen et al. 2006; Rodriguez et al. 2007; Bachmann and Bergantz 2008). As magmas ascend from the deepest part of the crust, they encounter cold wall rocks and tend to cool and quickly crystallize to the rheological locking point (~ 50 vol% crystals; Marsh 1981; Vigneresse et al. 1996). However, once they reach this intermediate crystallinity, the decreasing temperature differential with wall rocks, impeded convection, latent heat buffering, and periodic reheating from below will tend to keep the reservoir above its solidus (Marsh 1981; Koyaguchi and Kaneko 1999; Huber et al. 2009; Bea 2010) for significant lengths of time (up to >100,000 years, based on zircon growth histories; see Brown and Fletcher 1999; Vazquez and Reid 2002; Charlier et al. 2003; Vazquez and Reid 2004; Bachmann et al. 2007; Bindeman et al. 2008; Reid 2008). If this dacitic magma does not erupt at the surface (as it did for the Kefalos dacite) prior to reaching this rheological locking point, it will remain largely trapped in the upper crust. In such conditions, a cupola of evolved magma is likely to form by upward percolation of interstitial melt, ponding in the upper part of the magma reservoir (Bachmann and Bergantz 2004; Dufek and Bachmann 2010). In fairly warm upper crustal conditions that develop in long-lived provinces, reservoirs up to several thousands of km^3 may be generated (Jellinek and DePaolo 2003).

In the KNVC, a couple of lines of evidence support generation of the rhyolite by liquid extraction from a dacite mush. Firstly, the volcanic deposits show whole-rock compositional gaps (Buettner et al. 2005; Figs. 2, 5), while plagioclase compositions display a continuum that records the complete melt evolution for these upper crustal silicic magmas (Fig. 5). This compositional gap in the eruptive products (whole-rock), but *not* in the mineral chemistry, is predicted by the model of Dufek and Bachmann (2010), which implies *continuous crystallization but punctuated extraction* of discrete melt bodies from the source mush zones. Secondly, the P–T conditions of magma storage prior to eruption overlap between the dacite to rhyolite. Amphibole geothermobarometry indicates that the dacite, although initially crystallized at middle-crustal depths (at least 17 km depth; Fig. 10), follows a continuous polybaric crystallization path until storage in the upper crust prior to eruption. Magma chamber conditions for rhyodacites to high-silica rhyolites (extracted liquids) overlap with the lowest pressure and temperature estimates determined for the dacite.

Magmatic perturbation induced by caldera collapse

In the context of interstitial liquid extraction from upper crustal mushes, the reason for the changes in T, f_{O_2}, and composition from the Kefalos—KPT rhyolites and the Nisyros rhyodacites remains to be explained. As shown in Fig. 9, the eruption temperature measured by Fe–Ti oxides (and oxygen fugacity) increased by nearly 100°C immediately following the KPT eruption, and whole-rock and mineral chemistry indicate subtle changes in the crystallizing mineral assemblage (e.g., Nisyros magmas have higher Y, Zr than both rhyolites and dacites from Kefalos-KPT, but lower Sr for a given An content in plagioclase). In contrast, we note a more gradual return to KPT-type magmas (lower temperature, presence of quartz, biotite and sanidine) from Nisyros rhyodacites to Yali rhyolites (this paper and others; Francalanci et al. 1995; Buettner et al. 2005; Bachmann et al. 2007; Francalanci et al. 2007; Zellmer and Turner 2007; Pe-Piper and Moulton 2008; Bachmann 2010). These observations are best understood by modifying the upper crustal source zone of the rhyolitic magmas; the dacitic mush. We explore a couple of potential scenario below.

During growth of a silicic reservoir in the upper crust, the overpressure increases by 0.5 to 1 kb due to several internal and external factors (see for example Jellinek and DePaolo 2003; Karlstrom et al. 2009). Ultimately, the walls of the reservoir will fail, leading to an eruption (caldera-forming, if the reservoir is sufficiently large and shallow). In such conditions, much of the eruptible cap (magma with <50 vol% crystals) will be evacuated, while the remaining high-crystallinity, low-temperature mush zone will tend to quickly crystallize due to rapid depressurization and devolatilization (Fig. 11). Such a rapid decompression-induced crystallization would lead to a porphyritic texture with a fine-grained matrix and possibly granophyric intergrowth in the mush, a common observation in shallow plutonic sequences (e.g., Dilles 1987; du Bray and Pallister 1991; Candela 1997; Lipman et al. 1997; Wiebe et al. 2007; du Bray et al. 2010).

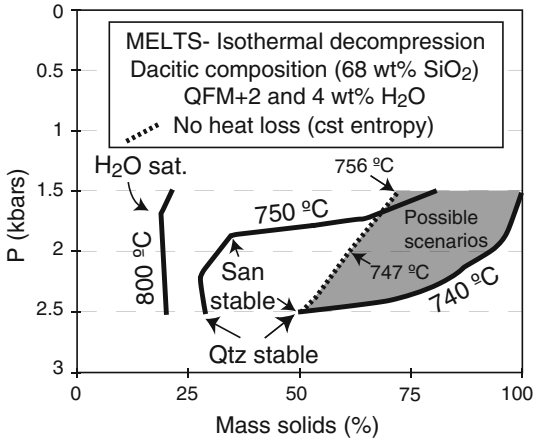

Fig. 11 MELTS simulations of a dacitic melt at different temperatures (800, 750, and 740°C), showing the sharp increase in crystallinity when the magma is suddenly decompressed at low temperature with quartz and sanidine present

Several characteristics of the KPT rhyolite indicate that a large decompression event (0.5–1 kb) during the eruption would have a significant quenching effect on the unerupted parts of the magma chamber (pressure quench of Tuttle and Bowen 1958). For this to happen, the unerupted magma leftover from the KPT eruption needed to be at a low temperature and crystal-rich, with a near-eutectic mineral assemblage (including quartz and sanidine; Fig. 11). On the basis of several observations, this was certainly the case. Firstly, the extraction of a rhyolitic melt from a crystal-rich intermediate progenitor is bound to leave behind a highly crystalline magma (approaching $\sim$>70 vol% crystals; Deering and Bachmann 2010). Secondly, the KPT rhyolite was indeed at low temperature, high crystallinity (up to 40 vol%) and had a near-eutectic mineral assemblage at the time of eruption. Hence, the unerupted parts had to have reached similar magmatic conditions and were likely to be at even higher crystallinity, as supported by the ubiquitous presence of comagmatic granitic enclaves with the same mineral assemblage and zircon U/Th/Pb ages in the KPT deposits (Keller 1969; Bachmann 2010).

Using MELTS-rhyolite (new version of MELTS specifically tuned for silicic compositions; Ghiorso and Sack 1995; Gualda et al. submitted), we have run several isothermal decompression simulations using a dacitic composition as a starting material at QFM + 2 and 4 wt% H_2O (Fig. 11). Once sanidine and quartz appear as phases in the simulations ($\leq$740°C), isothermal decompression leads to a nearly complete crystallization, even if the system overpressure is small (a 0.5 kb from 2.5 to 2 kb leads to a final crystallinity of >90 vol%; Fig. 11). However, these simulations ignore the effect of latent heat release during pressure quenching. Therefore, isentropic simulations (assuming no heat loss) were also run using MELTS-rhyolite. Such simulations show a $\sim$15°C increase in temperature and 20% increase in crystallinity for a decompression of 1 kb (from 2.5 to 1.5 kb). The isothermal and isentropic simulations constrain likely end-member scenarios in a natural setting. Therefore, a shallow, volatile-saturated, near-eutectic mush that is not erupted during a caldera collapse is likely to crystallize from $\geq$50–55 vol% to $\geq$70 vol% crystals in a short time after the decompression event.

On the basis of the predicted crystallinity increase following a large eruption, it should be expected that most of the source mush left-over in the crust will be too crystal-rich to ever be able to produce an eruptible high-SiO_2 rhyolite cap of significant size by melt extraction: It will effectively be forming a solidified pluton that will no longer be a significant part of the differentiating mush column. Hence, to generate highly evolved magmas in the same area postcaldera, a new upper crustal silicic reservoir has to grow from more mafic recharge from below. The most mafic volcanic rocks are predicted to erupt shortly after a caldera collapse, as the blocking cap of low-density silicic magma has been removed and/or stiffened. This is clearly observed in Nisyros, with the most mafic units (basaltic andesites and andesites) present at the lower stratigraphic levels (Volentik et al. 2006). The construction of a new upper crustal mush will be fed by incremental addition of intermediate (andesitic-dacitic) parents produced in the mid to lower crust (typically at 850–950°C). It will therefore start small and, assuming a constant recharge rate, will not be able to extract significant amounts of highly evolved interstitial melt over some period of time following the caldera collapse (a poorly constrained period, which depends on the magma production rate in a given area).

The hotter conditions in magmas following caldera collapse resulted in a pyroxene, plagioclase-rich, but amphibole, zircon-poor mineral assemblage. The presence of a higher modal content of anhydrous minerals suggests that the liquid extracted from a source mush for the Nisyros rhyodacites was relatively drier than the KPT-Kefalos magmas. The KPT rhyolite (and by extension Kefalos rhyolites) was certainly very water-rich (gas-saturated, with $\sim$4.5 to >6.5 wt% H_2O and 100–400 ppm CO_2 in quartz-hosted melt inclusions trapped at shallow depths; Bachmann et al. 2009). Unfortunately, Nisyros units do not carry mineral phases that efficiently trap melt inclusions and no direct water determinations were attempted. Using the plagioclase–liquid hygrometer (Lange 2009), the values for Nisyros rhyodacites (4.5–5 wt% H_2O at $\sim$850°C and 2.5 kb) are in close agreement with the Ridolfi et al. (2010) amphibole hygrometer and suggest a slightly lower water content than in the KPT-Kefalos rhyolites.

A lower dissolved water content in postcaldera intermediate magmas may be another consequence of the eruption-induced decompression event. As pressure is released during caldera collapse, the volatile saturation level will drop deeper in the magmatic column, depleting magmas in volatiles (including water). Using VolatileCalc (Newman and Lowenstern 2002) for a silicic magma with 5 wt% H_2O and 400 ppm CO_2 at 900°C in closed-system degassing with 2 wt% exsolved gas, a drop of 0.5 kb, typical of caldera collapse would remove ~0.5 wt% water from the system.

With time, the upper part of a reservoir is likely to stabilize at water-rich and cooler conditions as new recharge events add to the reservoir. As the reservoir becomes bigger, it will allow an evolved cap to accumulate at the roof (Bachmann and Bergantz 2004; Hildreth and Wilson 2007), thermally buffered (1) by the mass of crystal mush below, (2) by the high water content, and (3) by periodic recharge events whose primary effects are the reheating of the upper crustal mush (e.g., Pallister et al. 1992; Murphy et al. 2000; Bachmann et al. 2002; Bachmann 2010). Therefore, eruptions of crystal-poor magmas are expected to become more silicic and cooler with time, as is happening in the KNVC at present (Yali rhyolite; Fig. 12).

Another potential scenario involving independent liquid lines of descent beneath Kos and Nisyros (and a mixing of both for Yali magmas) cannot be completely ruled out. However, Nisyros volcano is situated on the southern edge of the KPT caldera (see Fig. 2 and Figure 2 of Pe-Piper and Moulton 2008). Therefore, some KPT magma were erupted from vents that are now underneath Nisyros. This close proximity in vent locations for at least some eruptions involving very distinctive magma types indicates that KPT and Nisyros reservoirs likely overlapped in space and that the petrologic differences originated from periodic variations in magma storage conditions rather than long-term disparity in source regions. In addition, having two independent volcanic systems would not provide any explanation for the observed petrologic changes throughout the KPT caldera cycle.

Conclusions

As it is typical for long-lived volcanic centers in subduction zones, the Aegean region of Kos—Nisyros (including the island of Yali and the Peninsula of Kefalos on Kos Island) displays a range of erupted magma types from basaltic andesite to high-SiO_2 rhyolites. This magmatic diversity is, in the Aegean and above other subduction zones, commonly attributed to chemical evolution by crystal fractionation accompanied by some assimilation of crustal material, either in the mantle (slab, sediment, crustal erosion) or by interaction with preexisting crust en route to the surface (e.g., Bowen 1928; Daly 1933; Di Paola 1974; Hawkesworth and Vollmer 1979; Taylor 1980; Briqueu et al. 1986; Mitropoulos et al. 1987; Druitt and Bacon 1989; Wyers and Barton 1989; Mitropoulos and Tarney 1992; Francalanci et al. 1995; Mitropoulos et al. 1998; Druitt et al. 1999; Gertisser and Keller 2003; Mortazavi and Sparks 2004; Jackson et al. 2007). Focusing on the evolved products (dacites to high-silica rhyolites), we have shown that major changes in mineralogy and temperature of erupted products occurred after the caldera collapse related to the KPT eruption. These changes, however, took place in a sequence of magmas that are related to each other by a simple liquid line of descent typical of a subduction zone (this paper and others; Francalanci et al. 1995; Buettner et al. 2005; Bachmann et al. 2007; Francalanci et al. 2007; Zellmer and Turner 2007; Pe-Piper and Moulton 2008; Bachmann 2010). Therefore,

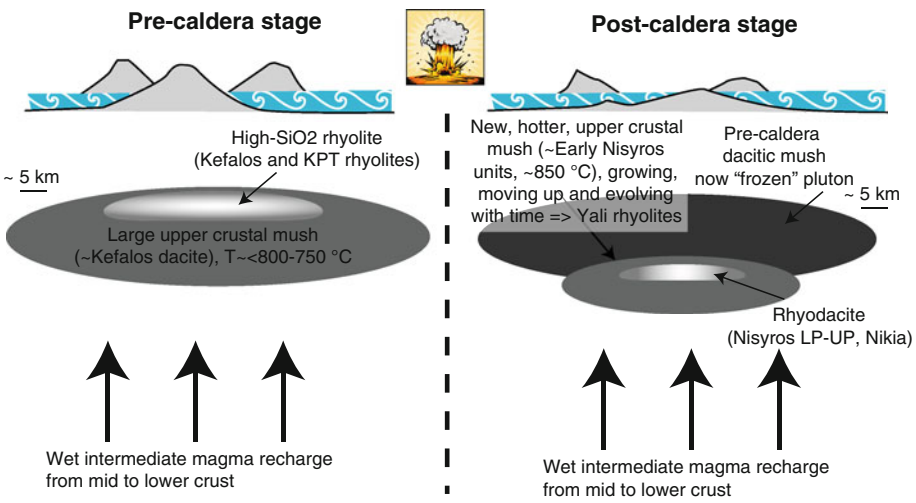

Fig. 12 Schematic illustration of the sequence of event that occurred prior to and after the KPT caldera collapse in the Kos-Nisyros volcanic center

we interpret the obvious mineralogical and P–T-f_{O_2} shifts not as a consequence of vastly different conditions in the source or in the deep part of the system, but rather as a modification of the silicic magma production zone in the upper part of the crust, most likely related to the caldera-forming eruption of the KPT. Such shifts in mineralogy and storage conditions of magmas following a major caldera collapse have been observed in other silicic centers around the world (e.g., Hildreth 2004; Shane et al. 2005), and strongly suggest that the two are related.

Acknowledgments This paper benefited from the help of a number of persons along the way, from logistical field support (G. Vougioukalakis and K. Kyriakopoulos) to efficient help in the lab (M. Grove with the Stanford-USGS SHRIMP analyses and C. Ginibre with the Lausanne microprobe) to providing constructive and insightful comments on this research (M. Dungan, B. Nelson, P. Lipman, T. Vogel, G. Bergantz, P. Ruprecht). We acknowledge funding from the Lombard fellowship (to Schnyder and Skopelitis), the Swiss National Science foundation (Swiss NSF grant 200021-111709/1 to Bachmann) and the US National Science foundation (NSF EAR grant 0809828 to Bachmann) during the final stages of this paper. We thank Georgia Pe-Piper and an anonymous reviewer for helpful comments on a previous version of this manuscript.

References

Aksu AE, Jenner G, Hiscott RN, Isler EB (2008) Occurrence, stratigraphy and geochemistry of Late Quaternary tephra layers in the Aegean Sea and the Marmara Sea. Mar Geol 252(3–4): 174–192

Allen SR (2001) Reconstruction of a major caldera-forming eruption from pyroclastic deposit characteristics: Kos Plateau Tuff, eastern Aegean Sea. J Volcanol Geotherm Res 105:141–162

Allen SR, McPhie J (2000) Water-settling and resedimentation of submarine rhyolitic pumice at Yali, eastern Aegean, Greece. J Volcanol Geotherm Res 95(1–4):285–307

Andersen DJ, Lindsley DH, Davidson PM (1993) QUILF: a PASCAL program to assess equilibria among Fe-Mg-Ti oxides, pyroxenes, olivine, and quartz. Comput Geosci 19:1333–1350

Annen C, Blundy JD, Sparks RSJ (2006) The genesis of intermediate and silicic magmas in deep crustal hot zones. J Petrol 47(3):505–539

Bachmann O (2010) The petrologic evolution and pre-eruptive conditions of the rhyolitic Kos Plateau Tuff (Aegean Arc). Cent Eur J Geosci. doi:10.2478/v10085-010-0009-4

Bachmann O, Bergantz GW (2004) On the origin of crystal-poor rhyolites: extracted from batholithic crystal mushes. J Petrol 45:1565–1582

Bachmann O, Bergantz GW (2008) Rhyolites and their source mushes across tectonic settings. J Petrol 49:2277–2285

Bachmann O, Dungan MA, Lipman PW (2002) The Fish Canyon magma body, San Juan volcanic field, Colorado: rejuvenation and eruption of an upper crustal batholith. J Petrol 43(8):1469–1503

Bachmann O, Charlier BLA, Lowenstern JB (2007) Zircon crystallization and recycling in the magma chamber of the rhyolitic Kos Plateau Tuff (Aegean Arc). Geology 35(1):73–76

Bachmann O, Wallace P, Bourquin J (2009) The melt inclusion record from the rhyolitic Kos Plateau Tuff (Aegean Arc). Contrib Mineral Petrol 159(2):187–202

Bachmann O, Schoene B, Schnyder C, Spikings R (2010) $^{40}Ar/^{39}Ar$ and U/Pb dating of young rhyolites in the Kos-Nisyros volcanic complex, Eastern Aegean Arc (Greece): age discordance due to excess 40Ar in biotite. Geochem Geophys Geosyst 11:Q0AA08. doi:10.1029/2010GC003073

Bacon RC, Hirschmann MM (1988) Mg/Mn partitioning as a test for equilibrium between coexisting Fe-Ti oxides. Am Mineral 73:57–61

Bea F (2010) Crystallization dynamics of granite magma chambers in the absence of regional stress: multiphysics modeling with natural examples. J Petrol 51(7):1541–1569

Bellon H, Jarrige JJ (1979) L'activité magmatique néogene et quaternaire dans l'ile de Kos, Greece: Données radiochronologiques. C R Acad Sci Paris 288:1359–1362

Bindeman IN, Valley JW (2001) Low-^{18}O rhyolites from Yellowstone: magmatic evolution based on zircons and individual phenocrysts. J Petrol 42:1491–1517

Bindeman IN, Fu B, Kita NT, Valley JW (2008) Origin and evolution of silicic magmatism at yellowstone based on ion microprobe analysis of isotopically zoned zircons. J Petrol 49(1):163–193

Bowen NL (1928) The evolution of igneous rocks. Dover publications, New York, p 332

Briqueu L, Javoy M, Lancelot JR, Tatsumoto M (1986) Isotope geochemistry of recent magmatism in the Aegean arc: Sr, Nd, Hf, and O isotopic ratios in the lavas of Milos and Santorini—geodynamic implications. Earth Planet Sci Lett 80:41–54

Brown SJA, Fletcher IR (1999) SHRIMP U-Pb dating of the preeruption growth history of zircons from the 340 ka Whakamaru Ignimbrite, New Zealand: evidence for >250 k.y. magma residence times. Geology 27(11):1035–1038

Buettner A, Kleinhanns IC, Rufer D, Hunziker JC, Villa IM (2005) Magma generation at the easternmost section of the Hellenic arc: Hf, Nd, Pb and Sr isotope geochemistry of Nisyros and Yali volcanoes (Greece). Lithos 83(1–2):29–46

Caliro S, Chiodini G, Galluzzo D, Granieri D, La Rocca M, Saccorotti G, Ventura G (2005) Recent activity of Nisyros volcano (Greece) inferred from structural, geochemical and seismological data. Bull Volcanol 67(4):358–369

Candela PA (1997) A review of shallow, ore-related granites: textures, volatiles, and ore metals. J Petrol 38(12):1619–1633

Charlier BLA, Peate DW, Wilson CJN, Lowenstern JB, Storey M, Brown SJA (2003) Crystallisation ages in coeval silicic magma bodies: 238U–230Th disequilibrium evidence from the Rotoiti and Earthquake Flat eruption deposits, Taupo Volcanic Zone, New Zealand. Earth Planet Sci Lett 206(3–4):441–457

Claiborne LE, Miller CF, Walker BA, Wooden JL, Mazdab FK, Bea F (2006) Tracking magmatic processes through Zr/Hf ratios in rocks and Hf and Ti zoning in zircons: an example from the Spirit Mountain batholith, Nevada. Mineral Mag 70:517–543

Claiborne L, Miller C, Wooden J (2010) Trace element composition of igneous zircon: a thermal and compositional record of the accumulation and evolution of a large silicic batholith, Spirit Mountain, Nevada. Contrib Mineral Petrol

Dabalakis P, Vougioukalakis G (1993) The Kefalos Tuff ring (W. Kos): depositional mechanisms, vent position, and model of the evolution of the eruptive activity. Bull Geol Soc Greece 28(2):259–273

Daly RA (1933) Igneous rocks and the depths of the Earth. McGraw Hill, New York

DePaolo DJ (1981) Trace element and isotopic effects of combined wallrock assimilation and fractional crystallization. Earth Planet Sci Lett 53:189–202

Di Paola GM (1974) Volcanology and petrology of Nisyros Island (Dodecanese, Greece). Bull Volcanol 38:944–987

Dilles JH (1987) The petrology of the Yerington batholith, Nevada: evidence for the evolution of porphyry copper ore fluids. Econ Geol 72:417–425

Druitt TH, Bacon CR (1989) Petrology of the zoned calcalkaline magma chamber of Mount Mazama, Crater Lake, Oregon. Contrib Mineral Petrol 101:245–259

Druitt TH, Edwards L, Mellors RM, Pyle DM, Sparks RSJ, Lanphere M, Davies M, Barriero B (1999) Santorini volcano, vol 19. Geological Society Memoir, London

du Bray EA, Pallister JS (1991) An ash flow caldera in cross section: ongoing field and geochemical studies of the mid-tertiary Turkey Creek Caldera, Chiricahua Mountains, SE Arizona. J Geophys Res 96(B8):13435–13457

du Bray EA, Bacon CR, John DA, Wooden JL, Mazdab FK (2010) Episodic intrusion, internal differentiation, and hydrothermal alteration of the Miocene Tatoosh intrusive suite south of Mount Rainier, Washington. Geological Society of America Bulletin

Dufek J, Bachmann O (2010) Quantum magmatism: magmatic compositional gaps generated by melt-crystal dynamics. Geology 38:687–690

Dufek J, Bergantz GW (2005) Lower crustal magma genesis and preservation: a stochastic framework for the evaluation of basalt—crust interaction. J Petrol 46:2167–2195

Francalanci L, Varekamp JC, Vougioukalakis G, Defant MJ, Innocenti F, Manetti P (1995) Crystal retention, fractionation and crustal assimilation in a convecting magma chamber, Nisyros Volcano, Greece. Bull Volcanol 56(8):601–620

Francalanci L, Varekamp JC, Vougioukalakis GE, Innocenti F, Manetti P (2007) Is there a compositional gap at Nisyros volcano? A comment on: magma generation at the easternmost section of the Hellenic arc: Hf, Nd, Pb and Sr isotope geochemistry of Nisyros and Yali volcanoes (Greece) [Lithos 83 (2005) 29–46]. Lithos 95(3–4):458–461

Fu B, Page FZ, Cavosie AJ, Fournelle J, Kita NT, Lackey JS, Wilde SA, Valley JW (2008) Ti-in-zircon thermometry: applications and limitations. Contrib Mineral Petrol 156:197–215

Gertisser R, Keller J (2003) Trace element and Sr, Nd, Pb and O isotope variations in medium-K and high-K volcanic rocks from Merapi volcano, Central Java, Indonesia: evidence for the involvement of subducted sediments in Sunda Arc Magma Genesis. J Petrol 44(3):457–489

Ghiorso MS, Evans BW (2008) Thermodynamics of rhombohedral oxide solid solutions and a revision of the Fe-Ti oxide geothermometer and oxygen-barometer. Am J Sci 308(9):957–1039

Ghiorso MS, Sack RO (1995) Chemical mass transfer in magmatic processes IV. A revised and internally consistent thermodynamic model for the interpolation and extrapolation of liquid–solid equilibria in magmatic systems at elevated temperatures and pressures. J Petrol 119:197–212

Gottsmann J, Rymer H, Wooler LK (2005) On the interpretation of gravity variations in the presence of active hydrothermal systems: Insights from the Nisyros Caldera, Greece. Geophys Res Lett 32:L23310

Gualda GAR, Ghiorso MS, Lemons RV, Carly TL (submitted) Rhyolite-MELTS: a modified calibration of MELTS optimized for silica-rich, fluid-bearing magmatic systems. J Petrol

Hawkesworth CJ, Vollmer R (1979) Crustal contamination versus enriched mantle: 143Nd/144Nd and 87Sr/86Sr evidence from the Italian volcanics. Contrib Mineral Petrol 69(2):151–165

Hildreth W (2004) Volcanological perspectives on Long Valley, Mammoth Mountain, and Mono Craters: several contiguous but discrete systems. J Volcanol Geotherm Res 136(3–4):169–198

Hildreth WS, Moorbath S (1988) Crustal contributions to arc magmatism in the Andes of Central Chile. Contrib Mineral Petrol 98:455–499

Hildreth WS, Wilson CJN (2007) Compositional zoning in the Bishop Tuff. J Petrol 48(5):951–999

Holland T, Blundy J (1994) Non-ideal interactions in calcic amphiboles and their bearing on amphibole-plagioclase thermometry. Contrib Mineral Petrol 116:433–447

Huber C, Bachmann O, Manga M (2009) Homogenization processes in silicic magma chambers by stirring and latent heat buffering. Earth Planet Sci Lett 283:38–47

Jackson J (1993) Rates of active deformation in the Eastern Mediterranean. In: Boschi E et al (eds) Recent evolution and seismicity of the mediterranean region. Kluwer, Dordrecht, pp 53–64

Jackson MG, Hart SR, Koppers AAP, Staudigel H, Konter J, Blusztajn J, Kurz M, Russell JA (2007) The return of subducted continental crust in Samoan lavas. Nature 448(7154):684–687

Jellinek AM, DePaolo DJ (2003) A model for the origin of large silicic magma chambers: precursors of caldera-forming eruptions. Bull Volcanol 65:363–381

Karlstrom L, Dufek J, Manga M (2009) Organization of volcanic plumbing through magmatic lensing by magma chambers and volcanic loads. J Geophys Res 114:B10204. doi:10.1029/2009JB006339

Keller J (1969) Origin of rhyolites by anatectic melting of granitic crustal rocks; the example of rhyolitic pumice from the island of Kos (Aegean sea). Bulletin Volcanologique 33(3):942–959

Koyaguchi T, Kaneko K (1999) A two-stage thermal evolution model of magmas in continental crust. J Petrol 40(2):241–254

Lagios E, Sakkas V, Parcharidis I, Dietrich V (2005) Ground deformation of Nisyros Volcano (Greece) for the period 1995–2002: results from DInSAR and DGPS observations. Bull Volcanol 68(2):201–214

Lange RA (2009) A thermodynamic model for the plagioclase-liquid hygrometer/thermometer. Am Mineral 94:494–506

Leake BE, Wooley AR, Arps CES, Birch WD, Gilbert MC, Grice JD, Hawthrone FC, Kato A, Kisch HJ, Krivovichev VG, Linthout K, Laird J, Mandarino JA, Maresch WV, Nickel EH, Rock NMS, Schumacher JC, Smith DC, Stephensen NCN, Ungaretti L, Whittaker EJW, Youzhi G (1997) Nomenclature of amphiboles: report of the subcommitee on amphiboles of the international mineralogical association, commission on new minerals and mineral names. Am Mineral 82:1019–1037

Limburg EM, Varekamp JC (1991) Young pumice deposits on Nisyros, Greece. Bull Volcanol 54(1):68–77

Lipman PW, Dungan MA, Bachmann O (1997) Comagmatic granophyric granite in the Fish Canyon Tuff, Colorado: implications for magma-chamber processes during a large ash-flow eruption. Geology 25(10):915–918

Longchamp C, Bonadonna C, Bachmann O, Skopelitis A (2011) Characterization of tephra deposits with limited exposure: the example of the two largest explosive eruptions at Nisyros volcano (Greece). Bull Volcanol 1–16. doi:10.1007/s00445-011-0469-9

Mann AC (1983) Trace element geochemistry of high alumina basalt—Andesite—Dacite—Rhyodacite lavas of the Main Volcanic Series of Santorini Volcano, Greece. Contrib Mineral Petrol 84(1):43–57

Marsh BD (1981) On the crystallinity, probability of occurrence, and rheology of lava and magma. Contrib Mineral Petrol 78:85–98

Matsuda J, Senoh K, Maruoka T, Sato H, Mitropoulos P (1999) K-Ar ages of the Aegean volcanic rocks and their implication for the arc-trench system. Geochem J 33:369–377

Mitropoulos P, Tarney J (1992) Significance of mineral composition variations in the Aegean Island Arc. J Volcanol Geotherm Res 51:283–303

Mitropoulos P, Tarney J, Saunders AD, Marsh NG (1987) Petrogenesis of Cenozoic rocks from the aegean island arc. J Volcanol Geotherm Res 32:177–193

Mitropoulos P, Tarney J, Stouraiti C, Notsu K, Arakawa Y (1998) Sr isotopic variations along the Aegean Arc: constraints on magma genesis on the basis of new Sr isotopic data. Bull Geol Soc Greece 32:225–230

Mortazavi M, Sparks RSJ (2004) Origin of rhyolite and rhyodacite lavas and associated mafic inclusions of Cape Akrotiri, Santorini: the role of wet basalt in generating calcalkaline silicic magmas. Contrib Mineral Petrol 146(4):397–413

Murphy MD, Sparks RSJ, Barclay J, Carroll MR, Brewer TS (2000) Remobilization of andesitic magma by intrusion of mafic magma at the Soufrière Hills Volcano, Montserrat, West Indies. J Petrol 41(1):21–42

Newman S, Lowenstern JB (2002) VolatileCalc: a silicate melt-H_2O-CO_2 solution model written in Visual Basic for excel. Comput Geosci 28(5):597–604

Pallister JS, Hoblitt RP, Reyes AG (1992) A basalt trigger for the 1991 eruptions of Pinatubo volcano? Nature 356:426–428

Papadopoulos GA, Sachpazi M, Panopoulou G, Stavrakakis G (1998) The volcanoseismic crisis of 1996–1997 in Nisyros, SE Aegean Sea, Greece. Terra Nova 10(3):151–154

Pasteels P, Kolios N, Boven A, Saliba E (1986) Applicability of the K/Ar method to whole-rock samples of acid lava and pumice: case of the Upper Pleistocene domes and pyroclasts on Kos Island, Aegean Sea, Greece. Chem Geol 57(1–2):145–154

Pe-Piper G, Moulton B (2008) Magma evolution in the Pliocene-Pleistocene succession of Kos, South Aegean arc (Greece). Lithos 106(1–2):110–124

Pe-Piper G, Piper DJW (2002) The igneous rocks of Greece. Gebrüder Borntreager, Berlin, p 573

Pe-Piper G, Piper DJW, Perissoratis C (2005) Neotectonics and the Kos Plateau Tuff eruption of 161 ka, South Aegean arc. J Volcanol Geotherm Res 139(3–4):315–338

Putirka K (2008) Thermometers and barometers for volcanic systems. In: Putirka K, Tepley F (eds) Minerals, inclusions and volcanic processes, vol 69. Reviews in Mineralogy and Geochemistry, Mineralogical Society of America, Washington, DC, pp 61–120

Reid MR (2008) How long to achieve supersize? Elements 4:23–28

Riciputi LR, Johnson CM, Sawyer DA, Lipman PW (1995) Crustal and magmatic evolution in a large multicyclic caldera complex: isotopic evidence from the central San Juan volcanic field. J Volcanol Geotherm Res 67:1–28

Ridolfi F, Renzulli A, Puerini M (2010) Stability and chemical equilibrium of amphibole in calc-alkaline magmas: an overview, new thermobarometric formulations and application to subduction-related volcanoes. Contrib Mineral Petrol 160(1):45–66

Rodriguez C, Selles D, Dungan M, Langmuir C, Leeman W (2007) Adakitic Dacites formed by intracrustal crystal fractionation of water-rich parent magmas at Nevado de Longavi Volcano (36.2 S; Andean Southern Volcanic Zone, Central Chile). J Petrol 48(11):2033–2061

Shane P, Smith V, Nairn I (2005) High temperature rhyodacites of the 36 ka Hauparu pyroclastic eruption, Okataina Volcanic Centre, New Zealand: Change in a silicic magmatic system following caldera collapse. J Volcanol Geotherm Res 147:357–376

Shimizu A, Sumino H, Nagao K, Notsu K, Mitropoulos P (2005) Variation in noble gas isotopic composition of gas samples from the Aegean arc, Greece. J Volcanol Geotherm Res 140(4):321–339

Smith PE, York D, Chen Y, Evensen NM (1996) Single crystal $^{40}Ar/^{39}Ar$ dating of a late Quaternary paroxysm on Kos, Greece; concordance of terrestrial and marine ages. Geophys Res Lett 23(21):3047–3050

Smith PE, Evensen NM, York D (2000) Under the volcano; a new dimension in Ar–Ar dating of volcanic ash. Geophys Res Lett 27(5):585–588

Taylor HP (1980) The effects of assimilation of country rocks by magmas on $^{18}O/^{16}O$ and $^{87}Sr/^{86}Sr$ systematics in igneous rocks. Earth Planet Sci Lett 47:243–254

Tuttle OF, Bowen NL (1958) Origin of granite in light of experimental studies in the system $NaAlSi_3O_8$-$KAlSi_3O_8$-SiO_2. Geol Soc Am Mem 74:153

Vanderkluysen L, Volentik A, Hernandez J, Hunziker JC, Bussy F, Principe C (2006a) The geology, geochemistry and evolution of Nisyros Volcano (Greece). Implications for the volcanic hazards. In: Hunziker JC, Marini L (eds) The petrology and geochemistry of lavas and tephras of Nisyros Volcano (Greece), vol 44. Mémoires de Géologie (Lausanne), Lausanne, p 192

Vanderkluysen L, Volentik A, Principe C, Hunziker JC, Hernandez J (2006b) Nisyros' volcanic evolution: the growth of a strato-volcano. In: Hunziker JC, Marini L (eds) The petrology and geochemistry of lavas and tephras of Nisyros Volcano (Greece), vol 44. Lausanne, Mémoires de Géologie (Lausanne), pp 100–106

Vazquez JA, Reid MR (2002) Time scales of magma storage and differentiation of voluminous high-silica rhyolites at Yellowstone caldera, Wyoming. Contrib Mineral Petrol 144(3):274–285

Vazquez JA, Reid MR (2004) Probing the accumulation history of the voluminous Toba Magma. Science 305:991–994

Vigneresse J-L, Barbey P, Cuney M (1996) Rheological transitions during partial melting and crystallization with application to felsic magma segregation and transfer. J Petrol 37(6):1579–1600

Volentik A, Vanderkluysen L, Principe C, Hunziker JC (2006) Stratigraphy of Nisyros vollcano (Greece). In: Hunziker JC, Marini L (eds) The geology, geochemistry and evolution of Nisyros Volcano (Greece). Implications for the volcanic hazards, vol 44. Mémoires de Géologie (Lausanne), pp 26-66

Wagner GJ, Storzer D, Keller J (1976) Spaltspurendatierungen quartarer Gesteinsglaser aus dem Mittelmeerraum. N Jb Miner Mh 2:84–94

Watson EB, Harrison TM (1983) Zircon saturation revisited: temperature and composition effects in a variety of crustal magma types. Earth Planet Sci Lett 64:295–304

Wiebe R, Wark D, Hawkins D (2007) Insights from quartz cathodoluminescence zoning into crystallization of the Vinalhaven granite, coastal Maine. Contrib Mineral Petrol 154(4):439–453

Wortel MJR, Spakman W (2000) Subduction and slab detachment in the Mediterranean-Carpathian Region. Science 290:1910–1917

Wyers GP, Barton M (1989) Polybaric evolution of calc-alkaline magmas from Nisyros, southeastern Hellenic Arc, Greece. J Petrol 30:1–37

Zellmer GF, Turner SP (2007) Arc dacite genesis pathways: evidence from mafic enclaves and their hosts in Aegean lavas. Lithos 95(3–4):346–362